Quartic Box-Spline Reconstruction on the BCC Lattice

Pacific Graphics 2012
(invited TVCG presentation)

Minho Kim

University of Seoul
School of Computer Science

13 Sep. 2012

Table of contents

Outline

Introduction

Introduction

Objective

An efficient reconstruction scheme for BCC volume datasets.

Introduction

Objective

An efficient reconstruction scheme for BCC volume datasets.

Contribution

- A novel reconstruction scheme with

Introduction

Objective

An efficient reconstruction scheme for BCC volume datasets.

Contribution

- A novel reconstruction scheme with
    - improved reconstruction quality and

Introduction

Objective

An efficient reconstruction scheme for BCC volume datasets.

Contribution

- A novel reconstruction scheme with
  - improved reconstruction quality and
  - faster evaluation on the CPU.

Introduction

Objective

An efficient reconstruction scheme for BCC volume datasets.

Contribution

- A novel reconstruction scheme with
    - improved reconstruction quality and
    - faster evaluation on the CPU.
- In-depth comparison and analysis of box-spline-based schemes.

Outline

Previous Work

Previous Work

- Box-spline-based reconstruction schemes

Previous Work

- Box-spline-based reconstruction schemes
  - Quartic 7-direction box-spline on the Cartesian lattice by Peters [1994]

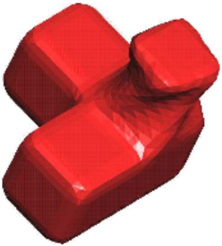

Previous Work

- Box-spline-based reconstruction schemes
  - Quartic 7-direction box-spline on the Cartesian lattice by Peters [1994]
  - Quintic 8-direction box-spline on the BCC lattice by Entezari et al. [2004]

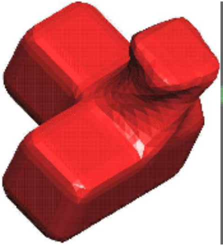

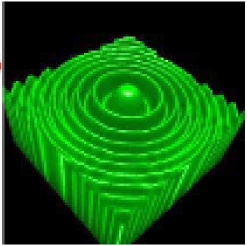

Previous Work

- Box-spline-based reconstruction schemes
  - Quartic 7-direction box-spline on the Cartesian lattice by Peters [1994]
  - Quintic 8-direction box-spline on the BCC lattice by Entezari et al. [2004]
  - Tri-cubic B-spline on the BCC lattice by Csébfalvi and Hadwiger [2006]

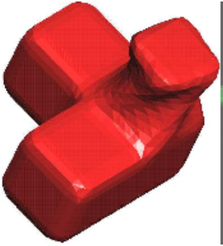
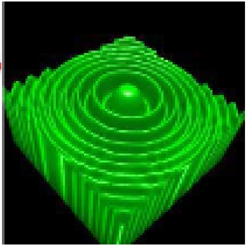
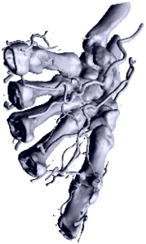

Previous Work

- Box-spline-based reconstruction schemes
  - Quartic 7-direction box-spline on the Cartesian lattice by Peters [1994]
  - Quintic 8-direction box-spline on the BCC lattice by Entezari et al. [2004]
  - Tri-cubic B-spline on the BCC lattice by Csébfalvi and Hadwiger [2006]
  - Cubic 6-direction box-spline on the FCC lattice by Kim et al. [2008]

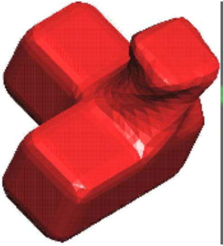
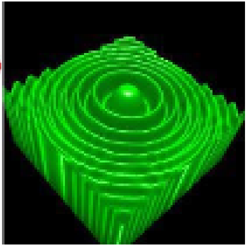
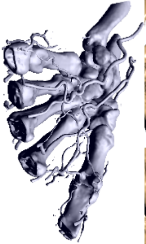
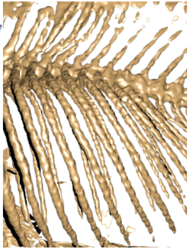

Outline

Volume Reconstruction

Volume Reconstruction

- Reconstructing a continuous signal from discrete dataset.

Volume Reconstruction

- Reconstructing a continuous signal from discrete dataset.
- Reconstruction filter + Sampling lattice

Volume Reconstruction

- Reconstructing a continuous signal from discrete dataset.
- Reconstruction filter + Sampling lattice
- The optimal sampling lattice is the dual of the densest sphere packing lattice. (Petersen and Middleton [1962])

Volume Reconstruction

- Reconstructing a continuous signal from discrete dataset.
- Reconstruction filter + Sampling lattice
- The optimal sampling lattice is the dual of the densest sphere packing lattice. (Petersen and Middleton [1962])
  $\rightarrow$ The optimal 3D sampling lattice is the BCC lattice.

Volume Reconstruction

- Reconstructing a continuous signal from discrete dataset.
- Reconstruction filter + Sampling lattice
- The optimal sampling lattice is the dual of the densest sphere packing lattice. (Petersen and Middleton [1962])
  $\rightarrow$ The optimal 3D sampling lattice is the BCC lattice.
- Efficient reconstruction filter?

Volume Reconstruction

- Reconstructing a continuous signal from discrete dataset.
- Reconstruction filter + Sampling lattice
- The optimal sampling lattice is the dual of the densest sphere packing lattice. (Petersen and Middleton [1962])
  $\rightarrow$ The optimal 3D sampling lattice is the BCC lattice.
- Efficient reconstruction filter? $\rightarrow$ Box-spline filters are good candidates.

The Body-Centered Cubic (BCC) Lattice

The Body-Centered Cubic (BCC) Lattice

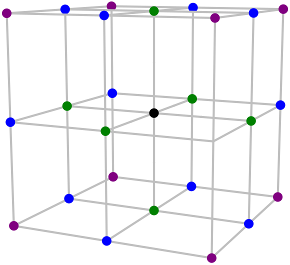

The Body-Centered Cubic (BCC) Lattice

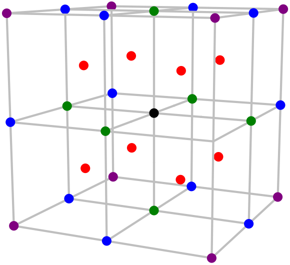

The Body-Centered Cubic (BCC) Lattice

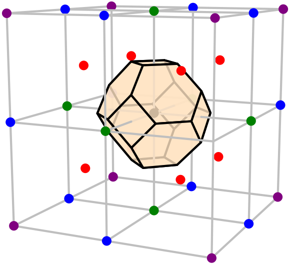

The Body-Centered Cubic (BCC) Lattice

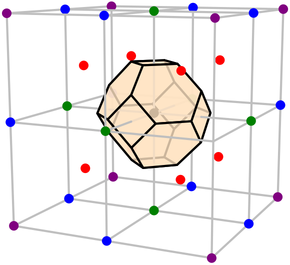

- The optimal 3D sampling lattice

The Body-Centered Cubic (BCC) Lattice

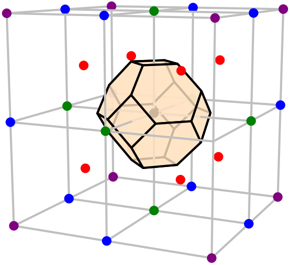

- The optimal 3D sampling lattice
- *Generator matrix*

$$\begin{bmatrix} -1 & 1 & 1 \\ 1 & -1 & 1 \\ 1 & 1 & -1 \end{bmatrix}$$

The Face-Centered Cubic (FCC) Lattice

The Face-Centered Cubic (FCC) Lattice

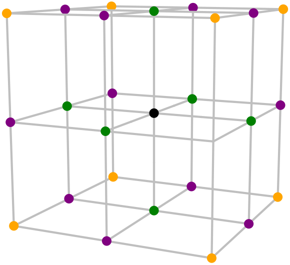

The Face-Centered Cubic (FCC) Lattice

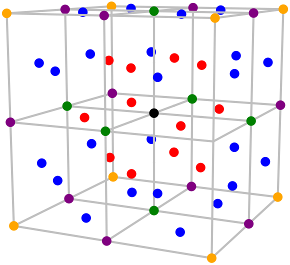

The Face-Centered Cubic (FCC) Lattice

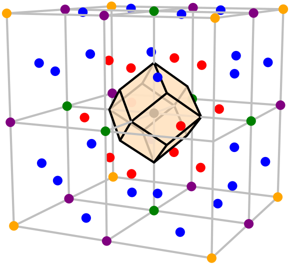

- Dual lattice of the BCC lattice

The Face-Centered Cubic (FCC) Lattice

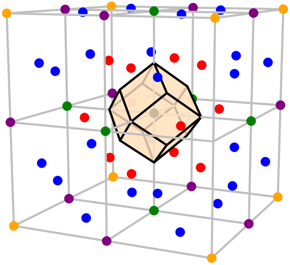

- Dual lattice of the BCC lattice $\rightarrow$ Sampling on the BCC lattice is equivalent to replicating spectrum on the FCC lattice.

The Face-Centered Cubic (FCC) Lattice

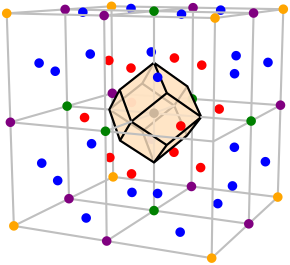

- Dual lattice of the BCC lattice $\rightarrow$ Sampling on the BCC lattice is equivalent to replicating spectrum on the FCC lattice.
- Generator matrix

$$\begin{bmatrix} 0 & 1 & 1 \\ 1 & 0 & 1 \\ 1 & 1 & 0 \end{bmatrix}$$

Box-Splines: Definition

Box-Splines: Definition

Direction matrix $\Xi = \begin{bmatrix} 1 & 0 & 1 & -1 \\ 0 & 1 & 1 & 1 \end{bmatrix}$

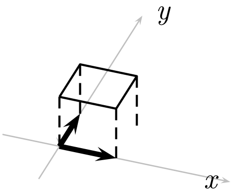

Box-Splines: Definition

Direction matrix $\Xi = \begin{bmatrix} 1 & 0 & 1 & -1 \\ 0 & 1 & 1 & 1 \end{bmatrix}$

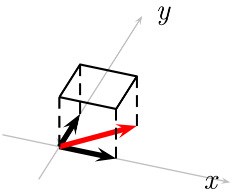

Box-Splines: Definition

Direction matrix $\Xi = \begin{bmatrix} 1 & 0 & 1 & -1 \\ 0 & 1 & 1 & 1 \end{bmatrix}$

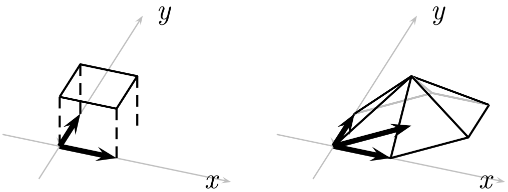

Box-Splines: Definition

Direction matrix $\Xi = \begin{bmatrix} 1 & 0 & 1 & -1 \\ 0 & 1 & 1 & 1 \end{bmatrix}$

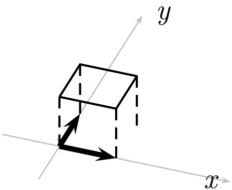

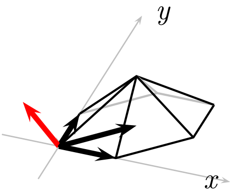

Box-Splines: Definition

Direction matrix $\Xi = \begin{bmatrix} 1 & 0 & 1 & -1 \\ 0 & 1 & 1 & 1 \end{bmatrix}$

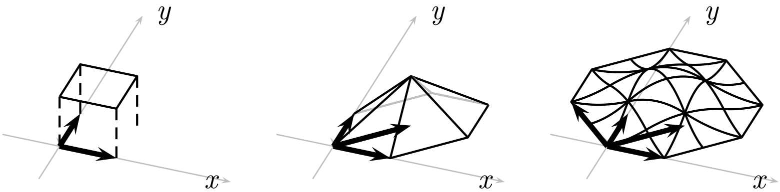

Box-Splines: Definition

Direction matrix $\Xi = \begin{bmatrix} 1 & 0 & 1 & -1 \\ 0 & 1 & 1 & 1 \end{bmatrix}$

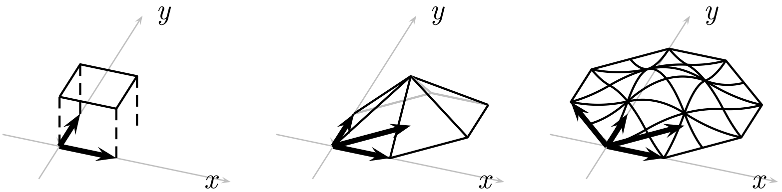

- Finite support defined by Minkowski sum of the directions.

Box-Splines: Definition

Direction matrix $\Xi = \begin{bmatrix} 1 & 0 & 1 & -1 \\ 0 & 1 & 1 & 1 \end{bmatrix}$

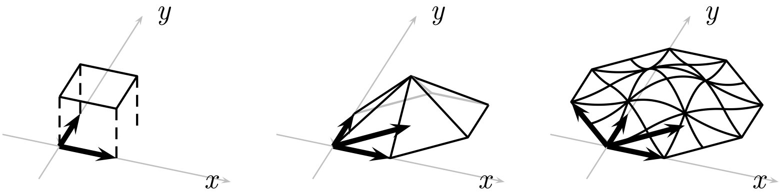

- Finite support defined by Minkowski sum of the directions.
- Piecewise polynomial of degree (# of directions - $\dim \operatorname{ran} \Xi$).

Box-Splines: Definition

Direction matrix $\Xi = \begin{bmatrix} 1 & 0 & 1 & -1 \\ 0 & 1 & 1 & 1 \end{bmatrix}$

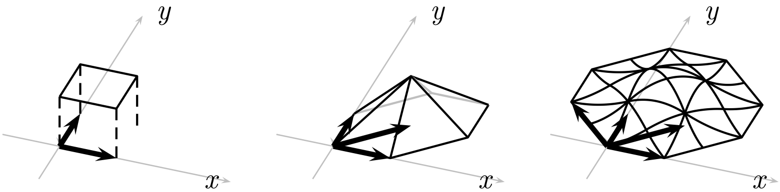

- Finite support defined by Minkowski sum of the directions.
- Piecewise polynomial of degree (# of directions - $\dim \operatorname{ran} \Xi$).
- Polynomial pieces are delineated by the shifts of the *knot planes* (Hyperplanes spanned by the directions of Ξ).

Box-Splines: Definition

Direction matrix $\Xi = \begin{bmatrix} 1 & 0 & 1 & -1 \\ 0 & 1 & 1 & 1 \end{bmatrix}$

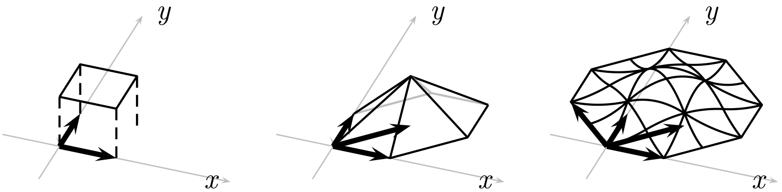

- Finite support defined by Minkowski sum of the directions.
- Piecewise polynomial of degree (# of directions - $\dim \operatorname{ran} \Xi$).
- Polynomial pieces are delineated by the shifts of the *knot planes* (Hyperplanes spanned by the directions of Ξ).
- Polynomial pieces join $C^{\rho(\Xi)-2}$.
  - $\rho(\Xi) := \min \# \boldsymbol{Z}$, $\boldsymbol{Z} \subset \Xi$, such that $\Xi \backslash \boldsymbol{Z}$ does not span $\mathbb{R}^n$.

Box-Splines: Reconstruction

Box-Splines: Reconstruction

- Convolution with a box-spline filter $M_{\boldsymbol{\Xi}}$:

$$\sum_{\boldsymbol{j} \in \boldsymbol{G}\mathbb{Z}^n} V(\boldsymbol{j}) M_{\boldsymbol{\Xi}}(\boldsymbol{x} - \boldsymbol{j}).$$

  - V: discrete dataset on $\boldsymbol{G}\mathbb{Z}^n$

Box-Splines: Reconstruction

- Convolution with a box-spline filter $M_{\boldsymbol{\Xi}}$:

$$\sum_{\boldsymbol{j} \in \boldsymbol{G}\mathbb{Z}^n} V(\boldsymbol{j}) M_{\boldsymbol{\Xi}}(\boldsymbol{x} - \boldsymbol{j}).$$

  - V: discrete dataset on $\boldsymbol{G}\mathbb{Z}^n$
- Evaluation at $\boldsymbol{x}$.

$$\sum_{\boldsymbol{j} \in \boldsymbol{G}\mathbb{Z}^n} V(\boldsymbol{j}) M_{\boldsymbol{\Xi}}(\boldsymbol{x} - \boldsymbol{j})$$

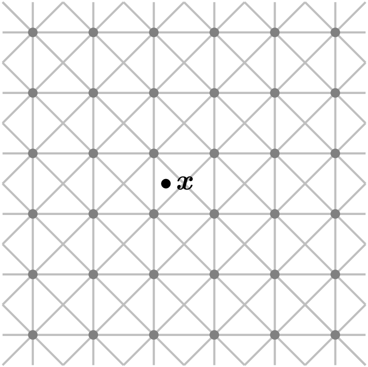

Box-Splines: Reconstruction

- Convolution with a box-spline filter M_{Ξ}:

$$\sum_{\boldsymbol{j} \in \boldsymbol{G}\mathbb{Z}^n} V(\boldsymbol{j}) M_{\Xi}(\boldsymbol{x} - \boldsymbol{j}).$$

  - V: discrete dataset on $\boldsymbol{G}\mathbb{Z}^n$
- Evaluation at $\boldsymbol{x}$.

$$\sum_{\boldsymbol{j} \in \boldsymbol{G}\mathbb{Z}^n} V(\boldsymbol{j}) M_{\Xi}(\boldsymbol{x} - \boldsymbol{j})$$

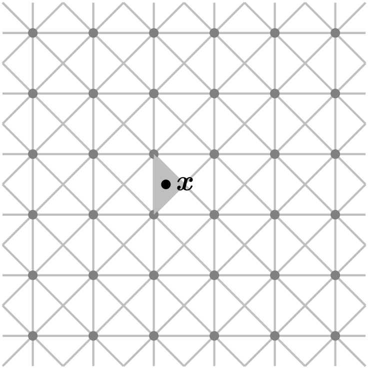

Box-Splines: Reconstruction

- Convolution with a box-spline filter M_{Ξ}:

$$\sum_{\boldsymbol{j} \in \boldsymbol{G}\mathbb{Z}^n} V(\boldsymbol{j}) M_{\Xi}(\boldsymbol{x} - \boldsymbol{j}).$$

  - V: discrete dataset on $\boldsymbol{G}\mathbb{Z}^n$
- Evaluation at $\boldsymbol{x}$.

$$\sum_{\boldsymbol{j} \in \boldsymbol{G}\mathbb{Z}^n} V(\boldsymbol{j}) M_{\Xi}(\boldsymbol{x} - \boldsymbol{j})$$
$$= V(\boldsymbol{j}_1) M_{\Xi}(\boldsymbol{x} - \boldsymbol{j}_1)$$

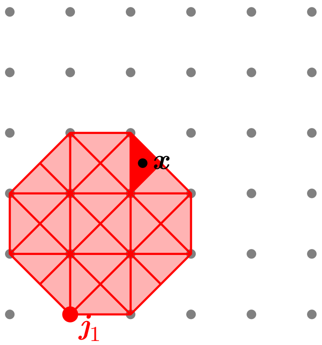

Box-Splines: Reconstruction

- Convolution with a box-spline filter M_{Ξ}:

$$\sum_{\boldsymbol{j} \in \boldsymbol{G}\mathbb{Z}^n} V(\boldsymbol{j}) M_{\Xi}(\boldsymbol{x} - \boldsymbol{j}).$$

  - V: discrete dataset on $\boldsymbol{G}\mathbb{Z}^n$

- Evaluation at $\boldsymbol{x}$.

$$\begin{aligned} &\sum_{\boldsymbol{j} \in \boldsymbol{G}\mathbb{Z}^n} V(\boldsymbol{j}) M_{\Xi}(\boldsymbol{x} - \boldsymbol{j}) \\ &= V(\boldsymbol{j}_1) M_{\Xi}(\boldsymbol{x} - \boldsymbol{j}_1) \\ &+ V(\boldsymbol{j}_2) M_{\Xi}(\boldsymbol{x} - \boldsymbol{j}_2) \end{aligned}$$

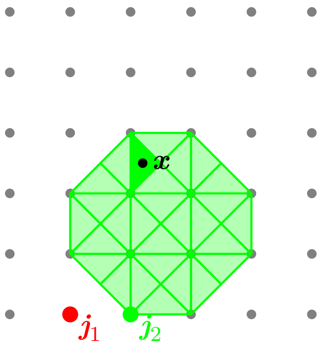

Box-Splines: Reconstruction

- Convolution with a box-spline filter M_{Ξ}:

$$\sum_{\boldsymbol{j} \in \boldsymbol{G}\mathbb{Z}^n} V(\boldsymbol{j}) M_{\Xi}(\boldsymbol{x} - \boldsymbol{j}).$$

  - V: discrete dataset on $\boldsymbol{G}\mathbb{Z}^n$
- Evaluation at $\boldsymbol{x}$.

$$\begin{aligned}
&\sum_{\boldsymbol{j} \in \boldsymbol{G}\mathbb{Z}^n} V(\boldsymbol{j}) M_{\Xi}(\boldsymbol{x} - \boldsymbol{j}) \\
&= V(\boldsymbol{j}_1) M_{\Xi}(\boldsymbol{x} - \boldsymbol{j}_1) \\
&+ V(\boldsymbol{j}_2) M_{\Xi}(\boldsymbol{x} - \boldsymbol{j}_2) \\
&+ V(\boldsymbol{j}_3) M_{\Xi}(\boldsymbol{x} - \boldsymbol{j}_3)
\end{aligned}$$

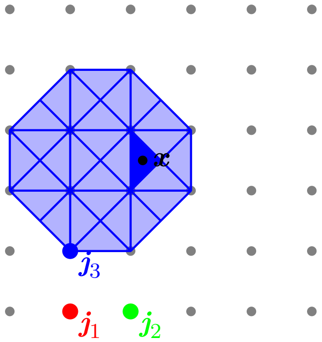

Box-Splines: Reconstruction

- Convolution with a box-spline filter M_{Ξ}:

$$\sum_{\boldsymbol{j} \in \boldsymbol{G}\mathbb{Z}^n} V(\boldsymbol{j}) M_{\Xi}(\boldsymbol{x} - \boldsymbol{j}).$$

  - V: discrete dataset on $\boldsymbol{G}\mathbb{Z}^n$
- Evaluation at $\boldsymbol{x}$.

$$\begin{aligned}
&\sum_{\boldsymbol{j} \in \boldsymbol{G}\mathbb{Z}^n} V(\boldsymbol{j}) M_{\Xi}(\boldsymbol{x} - \boldsymbol{j}) \\
&= V(\boldsymbol{j}_1) M_{\Xi}(\boldsymbol{x} - \boldsymbol{j}_1) \\
&+ V(\boldsymbol{j}_2) M_{\Xi}(\boldsymbol{x} - \boldsymbol{j}_2) \\
&+ V(\boldsymbol{j}_3) M_{\Xi}(\boldsymbol{x} - \boldsymbol{j}_3) \\
&+ V(\boldsymbol{j}_4) M_{\Xi}(\boldsymbol{x} - \boldsymbol{j}_4)
\end{aligned}$$

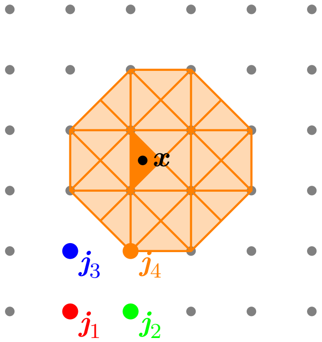

Box-Splines: Reconstruction

- Convolution with a box-spline filter M_{Ξ}:

$$\sum_{\boldsymbol{j} \in \boldsymbol{G}\mathbb{Z}^n} V(\boldsymbol{j}) M_{\Xi}(\boldsymbol{x} - \boldsymbol{j}).$$

  - V: discrete dataset on $\boldsymbol{G}\mathbb{Z}^n$
- Evaluation at $\boldsymbol{x}$.

$$\begin{aligned}
&\sum_{\boldsymbol{j} \in \boldsymbol{G}\mathbb{Z}^n} V(\boldsymbol{j}) M_{\Xi}(\boldsymbol{x} - \boldsymbol{j}) \\
&= V(\boldsymbol{j}_1) M_{\Xi}(\boldsymbol{x} - \boldsymbol{j}_1) \\
&+ V(\boldsymbol{j}_2) M_{\Xi}(\boldsymbol{x} - \boldsymbol{j}_2) \\
&+ V(\boldsymbol{j}_3) M_{\Xi}(\boldsymbol{x} - \boldsymbol{j}_3) \\
&+ V(\boldsymbol{j}_4) M_{\Xi}(\boldsymbol{x} - \boldsymbol{j}_4) \\
&+ V(\boldsymbol{j}_5) M_{\Xi}(\boldsymbol{x} - \boldsymbol{j}_5)
\end{aligned}$$

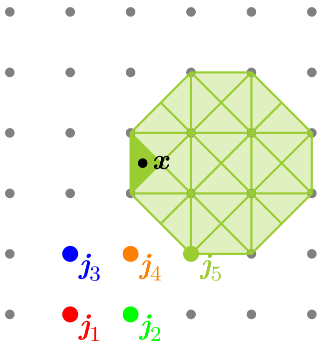

Box-Splines: Reconstruction

- Convolution with a box-spline filter M_{Ξ}:

$$\sum_{\boldsymbol{j} \in \boldsymbol{G}\mathbb{Z}^n} V(\boldsymbol{j}) M_{\Xi}(\boldsymbol{x} - \boldsymbol{j}).$$

  - V: discrete dataset on $\boldsymbol{G}\mathbb{Z}^n$
- Evaluation at $\boldsymbol{x}$.

$$\begin{aligned}
&\sum_{\boldsymbol{j} \in \boldsymbol{G}\mathbb{Z}^n} V(\boldsymbol{j}) M_{\Xi}(\boldsymbol{x} - \boldsymbol{j}) \\
&= V(\boldsymbol{j}_1) M_{\Xi}(\boldsymbol{x} - \boldsymbol{j}_1) \\
&+ V(\boldsymbol{j}_2) M_{\Xi}(\boldsymbol{x} - \boldsymbol{j}_2) \\
&+ V(\boldsymbol{j}_3) M_{\Xi}(\boldsymbol{x} - \boldsymbol{j}_3) \\
&+ V(\boldsymbol{j}_4) M_{\Xi}(\boldsymbol{x} - \boldsymbol{j}_4) \\
&+ V(\boldsymbol{j}_5) M_{\Xi}(\boldsymbol{x} - \boldsymbol{j}_5) \\
&+ V(\boldsymbol{j}_6) M_{\Xi}(\boldsymbol{x} - \boldsymbol{j}_6)
\end{aligned}$$

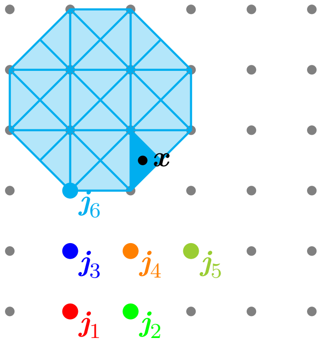

Box-Splines: Reconstruction

- Convolution with a box-spline filter M_Ξ:

$$\sum_{\boldsymbol{j} \in \boldsymbol{G}\mathbb{Z}^n} V(\boldsymbol{j}) M_\Xi(\boldsymbol{x} - \boldsymbol{j}).$$

  - V: discrete dataset on $\boldsymbol{G}\mathbb{Z}^n$
- Evaluation at $\boldsymbol{x}$.

$$\begin{aligned}
&\sum_{\boldsymbol{j} \in \boldsymbol{G}\mathbb{Z}^n} V(\boldsymbol{j}) M_\Xi(\boldsymbol{x} - \boldsymbol{j}) \\
&= V(\boldsymbol{j}_1) M_\Xi(\boldsymbol{x} - \boldsymbol{j}_1) \\
&+ V(\boldsymbol{j}_2) M_\Xi(\boldsymbol{x} - \boldsymbol{j}_2) \\
&+ V(\boldsymbol{j}_3) M_\Xi(\boldsymbol{x} - \boldsymbol{j}_3) \\
&+ V(\boldsymbol{j}_4) M_\Xi(\boldsymbol{x} - \boldsymbol{j}_4) \\
&+ V(\boldsymbol{j}_5) M_\Xi(\boldsymbol{x} - \boldsymbol{j}_5) \\
&+ V(\boldsymbol{j}_6) M_\Xi(\boldsymbol{x} - \boldsymbol{j}_6) \\
&+ V(\boldsymbol{j}_7) M_\Xi(\boldsymbol{x} - \boldsymbol{j}_7)
\end{aligned}$$

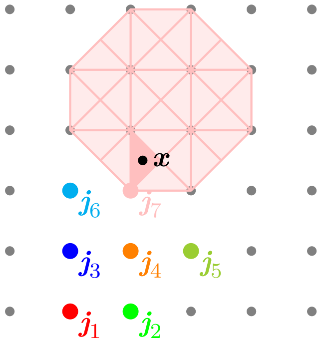

Box-Splines: Stencils

Box-Splines: Stencils

- Stencils: Relative data locations required for evaluating an input point.

Box-Splines: Stencils

- Stencils: Relative data locations required for evaluating an input point.
- Different stencil for each shift-invariant polynomial piece.

Box-Splines: Stencils

- Stencils: Relative data locations required for evaluating an input point.
- Different stencil for each shift-invariant polynomial piece.

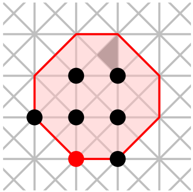

Box-Splines: Stencils

- Stencils: Relative data locations required for evaluating an input point.
- Different stencil for each shift-invariant polynomial piece.

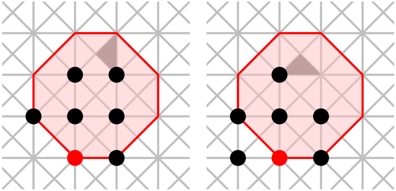

Box-Splines: Stencils

- Stencils: Relative data locations required for evaluating an input point.
- Different stencil for each shift-invariant polynomial piece.

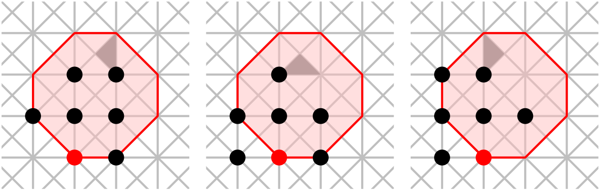

Box-Splines: Stencils

- Stencils: Relative data locations required for evaluating an input point.
- Different stencil for each shift-invariant polynomial piece.

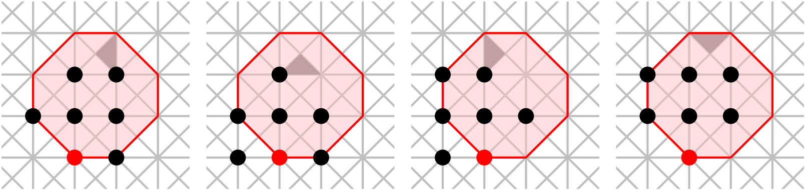

Box-Splines: Stencils

- Stencils: Relative data locations required for evaluating an input point.
- Different stencil for each shift-invariant polynomial piece.

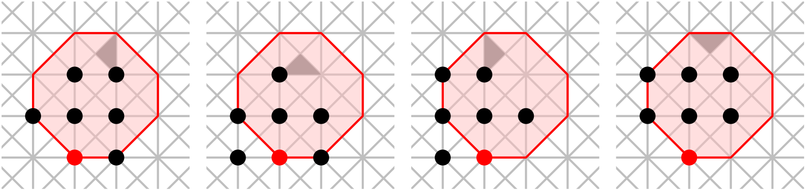

- Symmetric patterns for symmetric box-splines.

Box-Splines: Discrete Quasi-Interpolation Prefilter

Box-Splines: Discrete Quasi-Interpolation Prefilter

- Better approximation can be achieved by applying a *discrete quasi-interpolation prefilter* q beforehand:

Box-Splines: Discrete Quasi-Interpolation Prefilter

- Better approximation can be achieved by applying a *discrete quasi-interpolation prefilter* q beforehand:

$$\sum_{\boldsymbol{j} \in \boldsymbol{G}\mathbb{Z}^n} (V \star q)(\boldsymbol{j}) M_{\boldsymbol{\Xi}}(\boldsymbol{x} - \boldsymbol{j})$$

Box-Splines: Discrete Quasi-Interpolation Prefilter

- Better approximation can be achieved by applying a *discrete quasi-interpolation prefilter* q beforehand:

$$\sum_{\boldsymbol{j} \in \boldsymbol{G}\mathbb{Z}^n} (V \star q)(\boldsymbol{j}) M_{\boldsymbol{\Xi}}(\boldsymbol{x} - \boldsymbol{j})$$

  - $\star$: discrete convolution

$$(V \star q)(\boldsymbol{j}) := \sum_{\boldsymbol{k} \in \boldsymbol{G}\mathbb{Z}^n} V(\boldsymbol{k}) q(\boldsymbol{j} - \boldsymbol{k})$$

Box-Splines: Discrete Quasi-Interpolation Prefilter

- Better approximation can be achieved by applying a *discrete quasi-interpolation prefilter* q beforehand:

$$\sum_{\boldsymbol{j} \in \boldsymbol{G}\mathbb{Z}^n} (V \star q)(\boldsymbol{j}) M_{\boldsymbol{\Xi}}(\boldsymbol{x} - \boldsymbol{j})$$

  - $\star$: discrete convolution

$$(V \star q)(\boldsymbol{j}) := \sum_{\boldsymbol{k} \in \boldsymbol{G}\mathbb{Z}^n} V(\boldsymbol{k}) q(\boldsymbol{j} - \boldsymbol{k})$$

- Reduces the approximation order by annihilating all the lower terms of the Taylor expansion of the input signal.

Box-Splines: Summary

Box-Splines: Summary

- Lower (polynomial) degree than B-splines of the same approximation power

Box-Splines: Summary

- Lower (polynomial) degree than B-splines of the same approximation power
- Complicated spline evaluation

Box-Splines: Summary

- Lower (polynomial) degree than B-splines of the same approximation power
- Complicated spline evaluation $\rightarrow$ Can be simplified by leveraging symmetries.

Box-Splines: Summary

- Lower (polynomial) degree than B-splines of the same approximation power
- Complicated spline evaluation $\rightarrow$ Can be simplified by leveraging symmetries.
- Can be easily constructed on non-Cartesian lattices using lattice directions.

Box-Splines: Summary

- Lower (polynomial) degree than B-splines of the same approximation power
- Complicated spline evaluation $\rightarrow$ Can be simplified by leveraging symmetries.
- Can be easily constructed on non-Cartesian lattices using lattice directions.
- “Box Splines” by de Boor et al. [1993]

Outline

Box-Spline Filters

Box-Spline Filters

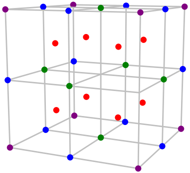

Box-Spline Filters

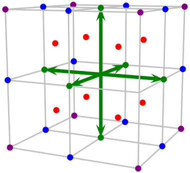

bcc12 [1]

[1] Tri-cubic B-spline by Csébfalvi and Hadwiger [2006]

Box-Spline Filters

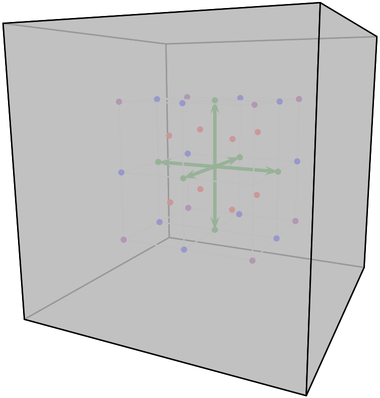

bcc12 [1]

[1] Tri-cubic B-spline by Csébfalvi and Hadwiger [2006]

Box-Spline Filters

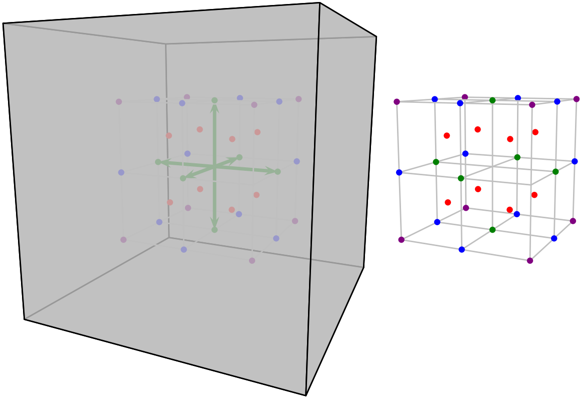

bcc12 [1]

[1] Tri-cubic B-spline by Csébfalvi and Hadwiger [2006]

Box-Spline Filters

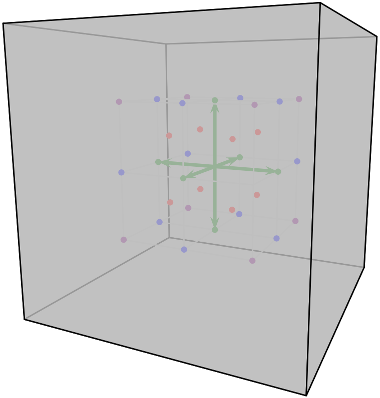

bcc12 [1]

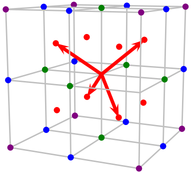

bcc8 [2]

[1] Tri-cubic B-spline by Csébfalvi and Hadwiger [2006]

[2] 8-direction box-spline by Entezari et al. [2004]

Box-Spline Filters

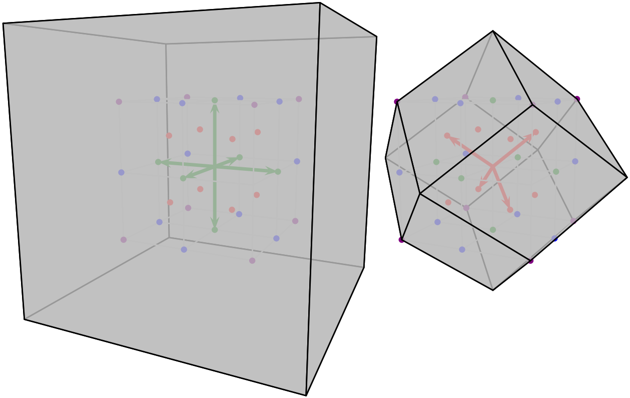

bcc12 [1] bcc8 [2]

[1] Tri-cubic B-spline by Csébfalvi and Hadwiger [2006]

[2] 8-direction box-spline by Entezari et al. [2004]

Box-Spline Filters

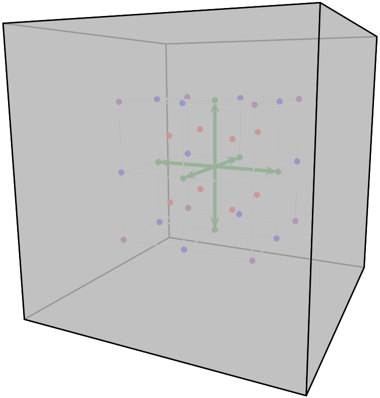

bcc12 [1]

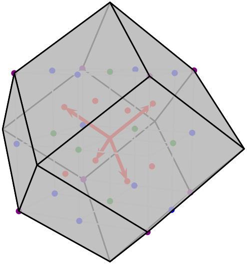

bcc8 [2]

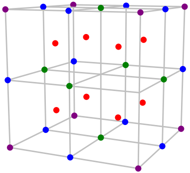

[1] Tri-cubic B-spline by Csébfalvi and Hadwiger [2006]

[2] 8-direction box-spline by Entezari et al. [2004]

Box-Spline Filters

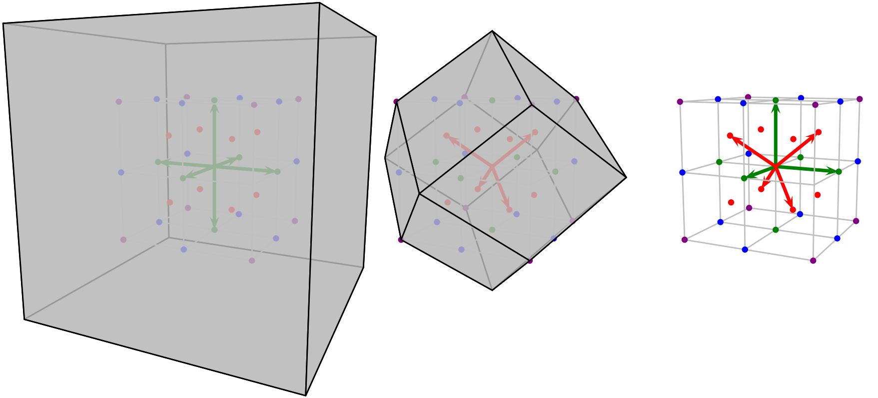

bcc12 [1] bcc8 [2] bcc7[3]

[1] Tri-cubic B-spline by Csébfalvi and Hadwiger [2006]

[2] 8-direction box-spline by Entezari et al. [2004]

[3] This work

Box-Spline Filters

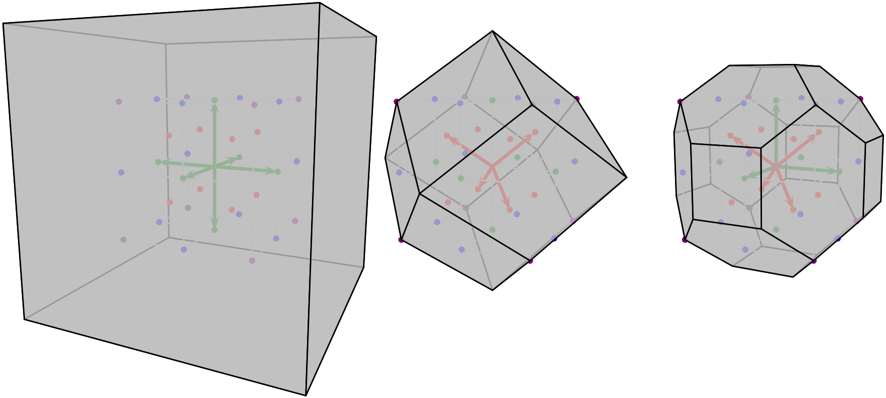

bcc12 [1] bcc8 [2] bcc7[3]

[1] Tri-cubic B-spline by Csébfalvi and Hadwiger [2006]

[2] 8-direction box-spline by Entezari et al. [2004]

[3] This work

BCC Volume Reconstruction Schemes

BCC Volume Reconstruction Schemes

Filter	bcc12	bcc8	bcc7

BCC Volume Reconstruction Schemes

Filter	bcc12	bcc8	bcc7
Approximation order	4	4	4

BCC Volume Reconstruction Schemes

Filter	bcc12	bcc8	bcc7
Approximation order	4	4	4
(Polynomial) Degree	9	5	4

BCC Volume Reconstruction Schemes

Filter	bcc12	bcc8	bcc7
Approximation order	4	4	4
(Polynomial) Degree	9	5	4
Volume of support	512	128	120

BCC Volume Reconstruction Schemes

Filter	bcc12	bcc8	bcc7
Approximation order	4	4	4
(Polynomial) Degree	9	5	4
Volume of support	512	128	120
Stencil size	128	32	30

BCC Volume Reconstruction Schemes

Filter	bcc12	bcc8	bcc7
Approximation order	4	4	4
(Polynomial) Degree	9	5	4
Volume of support	512	128	120
Stencil size	128	32	30
Riesz basis?	no	yes	no

Level Sets (bcc8 vs. bcc7)

Level Sets (bcc8 vs. bcc7)

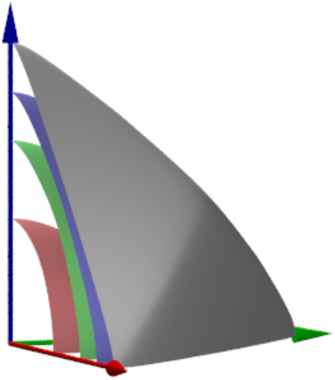

bcc8

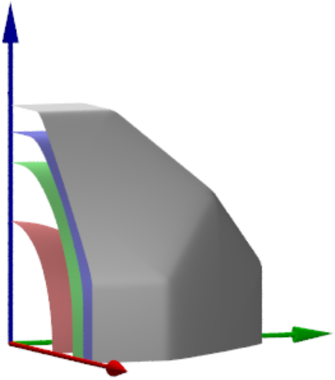

bcc7

- Level sets of 10^{-1}, 10^{-2}, 10^{-3}, and 10^{-5}.

Knot Planes

Knot Planes

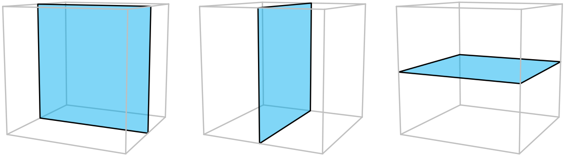

Knot Planes

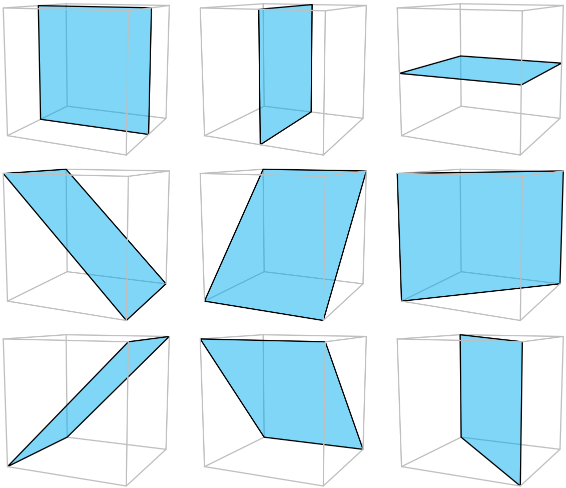

Polynomial Structure

Polynomial Structure

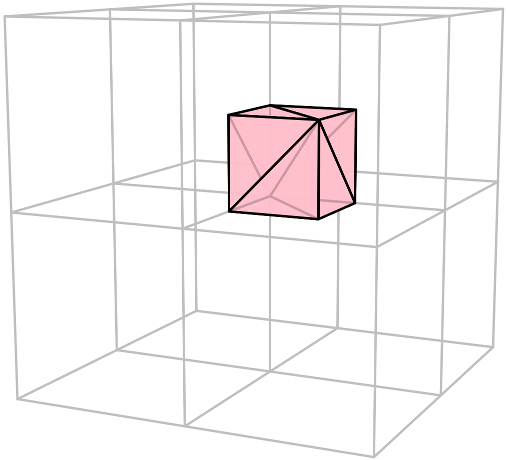

$$2\mathbb{Z}^3 + (0, 0, 0) + [0, 1]^3$$

$$2\mathbb{Z}^3 + (1, 1, 1) + [0, 1]^3$$

Polynomial Structure

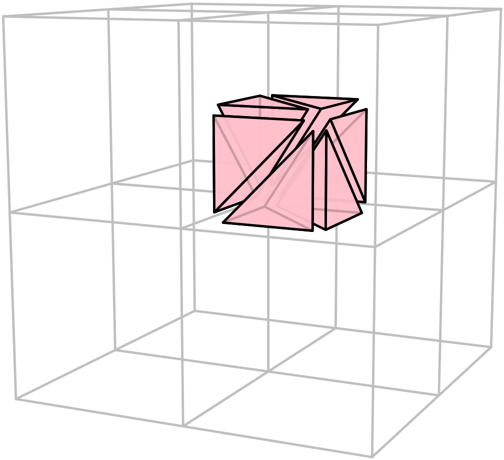

$$2\mathbb{Z}^3 + (0, 0, 0) + [0, 1]^3$$

$$2\mathbb{Z}^3 + (1, 1, 1) + [0, 1]^3$$

Polynomial Structure

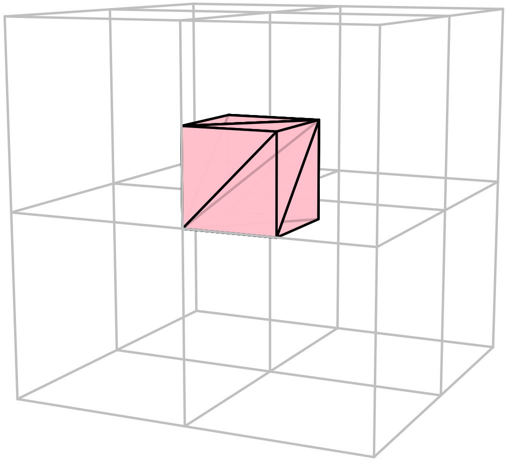

$$2\mathbb{Z}^3 + (1,0,0) + [0,1]^3$$

$$2\mathbb{Z}^3 + (0,1,1) + [0,1]^3$$

Polynomial Structure

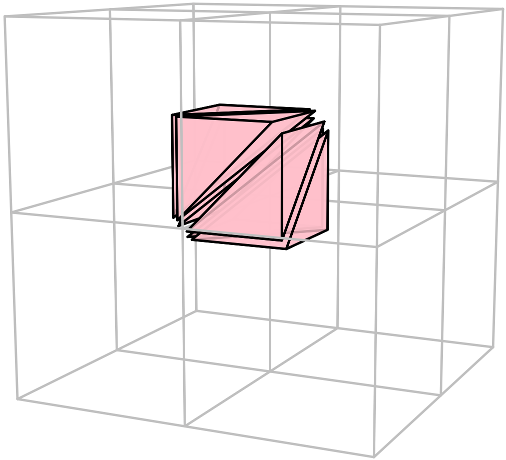

$$2\mathbb{Z}^3 + (1,0,0) + [0,1]^3$$

$$2\mathbb{Z}^3 + (0,1,1) + [0,1]^3$$

Polynomial Structure

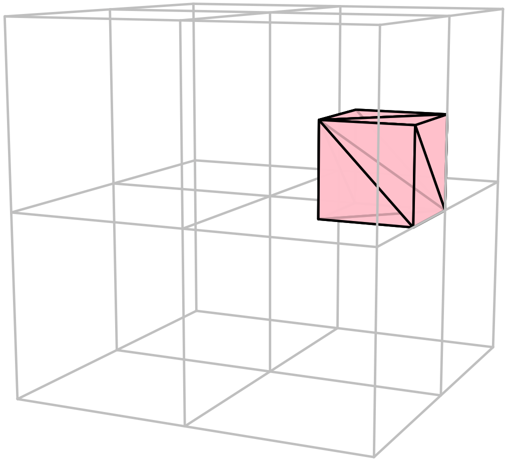

$$2\mathbb{Z}^3 + (0, 1, 0) + [0, 1]^3$$

$$2\mathbb{Z}^3 + (1, 0, 1) + [0, 1]^3$$

Polynomial Structure

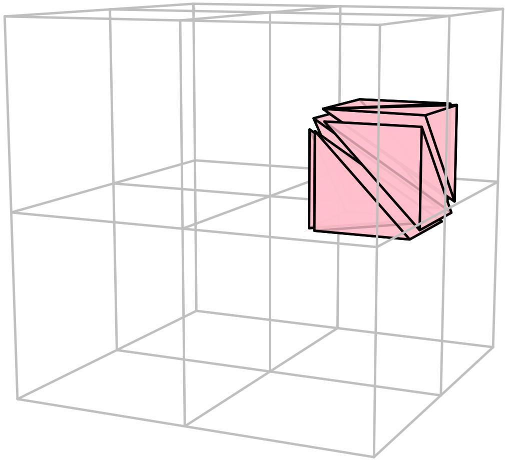

$$2\mathbb{Z}^3 + (0, 1, 0) + [0, 1]^3$$

$$2\mathbb{Z}^3 + (1, 0, 1) + [0, 1]^3$$

Polynomial Structure

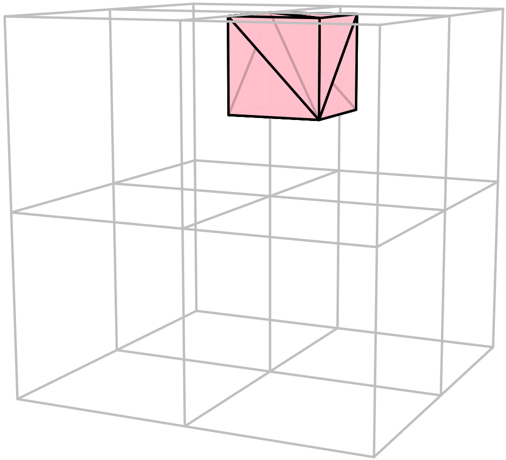

$$2\mathbb{Z}^3 + (0,0,1) + [0,1]^3$$

$$2\mathbb{Z}^3 + (1,1,0) + [0,1]^3$$

Polynomial Structure

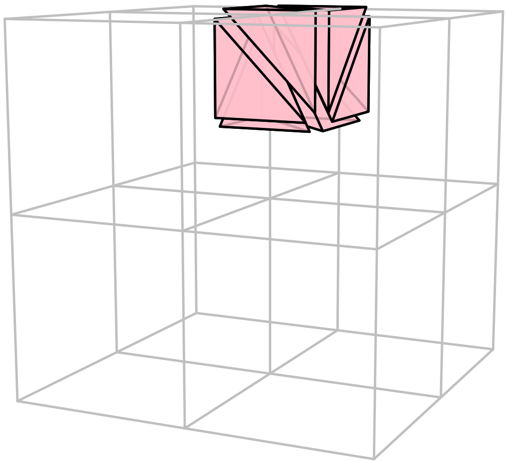

$$2\mathbb{Z}^3 + (0,0,1) + [0,1]^3$$

$$2\mathbb{Z}^3 + (1,1,0) + [0,1]^3$$

Stencil

Stencil

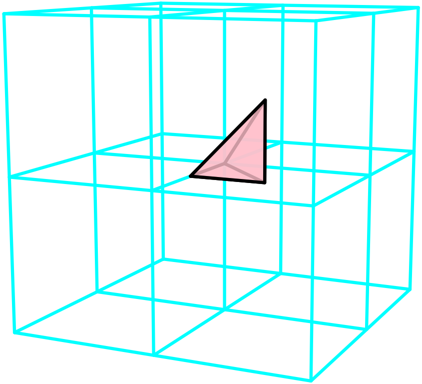

- *Reference tetrahedron* with vertices $\{(0,0,0),(1,0,0),(1,1,0),(1,1,1)\}$.

Stencil

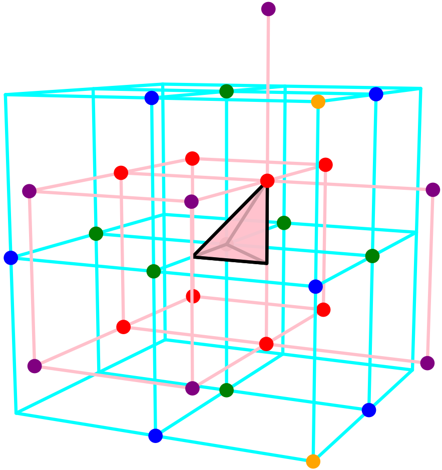

- *Reference tetrahedron* with vertices $\{(0,0,0),(1,0,0),(1,1,0),(1,1,1)\}$.
- 30 data values are required for evaluation.

Evaluation of a Spline

Evaluation of a Spline

function EvaluateQuartic(V, x)

Evaluation of a Spline

function EvaluateQuartic(V, x)

Find the reflection matrix $\boldsymbol{R}$ that maps the cube of type $\boldsymbol{k} := (\lfloor \boldsymbol{x} \rfloor \text{ modulo } 2)$ to the cube containing the reference tetrahedron.

Evaluation of a Spline

function EvaluateQuartic(V, x)

Find the reflection matrix $\boldsymbol{R}$ that maps the cube of type $\boldsymbol{k} := (\lfloor \boldsymbol{x} \rfloor \text{ modulo } 2)$ to the cube containing the reference tetrahedron.

Find (among six) the tetrahedron containing $\boldsymbol{R}(\boldsymbol{x} - \lfloor \boldsymbol{x} \rfloor)$ by testing against three knot planes inside the cube.

Evaluation of a Spline

function EvaluateQuartic(V, x)

Find the reflection matrix $\boldsymbol{R}$ that maps the cube of type $\boldsymbol{k} := (\lfloor \boldsymbol{x} \rfloor \text{ modulo } 2)$ to the cube containing the reference tetrahedron.

Find (among six) the tetrahedron containing $\boldsymbol{R}(\boldsymbol{x} - \lfloor \boldsymbol{x} \rfloor)$ by testing against three knot planes inside the cube.

Find the permutation matrix $\boldsymbol{P}$ that maps the tetrahedron to the reference tetrahedron.

Evaluation of a Spline

function EvaluateQuartic(V, x)

Find the reflection matrix $\boldsymbol{R}$ that maps the cube of type $\boldsymbol{k} := (\lfloor \boldsymbol{x} \rfloor \text{ modulo } 2)$ to the cube containing the reference tetrahedron.

Find (among six) the tetrahedron containing $\boldsymbol{R}(\boldsymbol{x} - \lfloor \boldsymbol{x} \rfloor)$ by testing against three knot planes inside the cube.

Find the permutation matrix $\boldsymbol{P}$ that maps the tetrahedron to the reference tetrahedron.

$\dot{\boldsymbol{x}} \leftarrow \boldsymbol{PR}(\boldsymbol{x} - \lfloor \boldsymbol{x} \rfloor)$

Evaluation of a Spline

function EvaluateQuartic(V, $\boldsymbol{x}$)

Find the reflection matrix $\boldsymbol{R}$ that maps the cube of type $\boldsymbol{k} := (\lfloor \boldsymbol{x} \rfloor \text{ modulo } 2)$ to the cube containing the reference tetrahedron.

Find (among six) the tetrahedron containing $\boldsymbol{R}(\boldsymbol{x} - \lfloor \boldsymbol{x} \rfloor)$ by testing against three knot planes inside the cube.

Find the permutation matrix $\boldsymbol{P}$ that maps the tetrahedron to the reference tetrahedron.

$\dot{\boldsymbol{x}} \leftarrow \boldsymbol{PR}(\boldsymbol{x} - \lfloor \boldsymbol{x} \rfloor)$

for $i = 1$ to 30 **do**

Evaluation of a Spline

function EvaluateQuartic(V, $\boldsymbol{x}$)

Find the reflection matrix $\boldsymbol{R}$ that maps the cube of type $\boldsymbol{k} := (\lfloor \boldsymbol{x} \rfloor$ modulo $2)$ to the cube containing the reference tetrahedron.

Find (among six) the tetrahedron containing $\boldsymbol{R}(\boldsymbol{x} - \lfloor \boldsymbol{x} \rfloor)$ by testing against three knot planes inside the cube.

Find the permutation matrix $\boldsymbol{P}$ that maps the tetrahedron to the reference tetrahedron.

$\dot{\boldsymbol{x}} \leftarrow \boldsymbol{P}\boldsymbol{R}(\boldsymbol{x} - \lfloor \boldsymbol{x} \rfloor)$

for $i = 1$ to 30 **do**

$\boldsymbol{j} \leftarrow \mathcal{J}_7(i)$

Evaluation of a Spline

function EvaluateQuartic(V, $\boldsymbol{x}$)

Find the reflection matrix $\boldsymbol{R}$ that maps the cube of type $\boldsymbol{k} := (\lfloor \boldsymbol{x} \rfloor \text{ modulo } 2)$ to the cube containing the reference tetrahedron.

Find (among six) the tetrahedron containing $\boldsymbol{R}(\boldsymbol{x} - \lfloor \boldsymbol{x} \rfloor)$ by testing against three knot planes inside the cube.

Find the permutation matrix $\boldsymbol{P}$ that maps the tetrahedron to the reference tetrahedron.

$\dot{\boldsymbol{x}} \leftarrow \boldsymbol{PR}(\boldsymbol{x} - \lfloor \boldsymbol{x} \rfloor)$

for $i = 1$ to 30 **do**

$\boldsymbol{j} \leftarrow \mathcal{J}_7(i)$

$c_i \leftarrow V(\boldsymbol{k} + (\boldsymbol{PR})^{-1}\boldsymbol{j})$

end for

Evaluation of a Spline

function EvaluateQuartic(V, $\boldsymbol{x}$)

Find the reflection matrix $\boldsymbol{R}$ that maps the cube of type $\boldsymbol{k} := (\lfloor \boldsymbol{x} \rceil \text{ modulo } 2)$ to the cube containing the reference tetrahedron.

Find (among six) the tetrahedron containing $\boldsymbol{R}(\boldsymbol{x} - \lfloor \boldsymbol{x} \rceil)$ by testing against three knot planes inside the cube.

Find the permutation matrix $\boldsymbol{P}$ that maps the tetrahedron to the reference tetrahedron.

$\dot{\boldsymbol{x}} \leftarrow \boldsymbol{PR}(\boldsymbol{x} - \lfloor \boldsymbol{x} \rceil)$

for $i = 1$ to 30 **do**

$\boldsymbol{j} \leftarrow \mathcal{J}_7(i)$

$c_i \leftarrow V(\boldsymbol{k} + (\boldsymbol{PR})^{-1}\boldsymbol{j})$

end for

Evaluate the constructed polynomial piece.

end function

Outline

CPU Evaluation Time

CPU Evaluation Time

- 10^7 points randomly generated inside each volume.

CPU Evaluation Time

- 10^7 points randomly generated inside each volume.
- System specifications:
  - Ubuntu 11.04/
  - quad-core Intel® Xeon® CPU X5550 @2.67GHz with L2 Cache 8MB/
  - 6GB main memory)

CPU Evaluation Time

- 10^7 points randomly generated inside each volume.
- System specifications:
  - Ubuntu 11.04/
  - quad-core Intel® Xeon® CPU X5550 @2.67GHz with L2 Cache 8MB/
  - 6GB main memory)

dataset	bcc12	bcc8 (t_8)	bcc7 (t_7)	t_7/t_8 (%)
$21^3 \times 2$	3.83445	2.09095	1.55458	74.3
$27^3 \times 2$	4.24062	2.24015	1.69082	75.5
$32^3 \times 2$	4.31606	2.29917	1.75987	76.5
$37^3 \times 2$	4.43997	2.35084	1.79927	76.5
$45^3 \times 2$	4.41845	2.35842	1.84051	78.0
$57^3 \times 2$	4.58235	2.42169	1.88100	77.7
$77^3 \times 2$	6.46921	3.24693	2.66483	82.1
$93^3 \times 2$	7.26688	3.61189	2.98389	82.6
$117^3 \times 2$	7.82863	3.91083	3.18585	81.5

- in seconds

Integral Filter Metrics

Integral Filter Metrics

- Proposed by Marschner and Lobb [1994]

Integral Filter Metrics

- Proposed by Marschner and Lobb [1994]
- Smoothing metric

$$S(\phi) := 1 - \frac{1}{|N_n|} \int_{N_n} |\widehat{\phi}|^2 \, dV$$

Integral Filter Metrics

- Proposed by Marschner and Lobb [1994]
- Smoothing metric

$$S(\phi) := 1 - \frac{1}{|N_n|} \int_{N_n} |\widehat{\phi}|^2 dV$$

- Post-aliasing metric

$$P(\phi) := \frac{1}{|N_n|} \int_{\overline{N_n}} |\widehat{\phi}|^2 dV$$

Integral Filter Metrics

- Proposed by Marschner and Lobb [1994]
- Smoothing metric

$$S(\phi) := 1 - \frac{1}{|N_n|} \int_{N_n} |\widehat{\phi}|^2 \, dV$$

- Post-aliasing metric

$$P(\phi) := \frac{1}{|N_n|} \int_{\overline{N_n}} |\widehat{\phi}|^2 \, dV$$

filter	smoothing	post-aliasing
bcc12	0.94495	0.00004
bcc8	0.85287	0.00399
bcc7	0.85488	0.00355

Spectra Visualization

Spectra Visualization

- Spectra evaluated on three planes on the FCC lattice in the frequency domain.

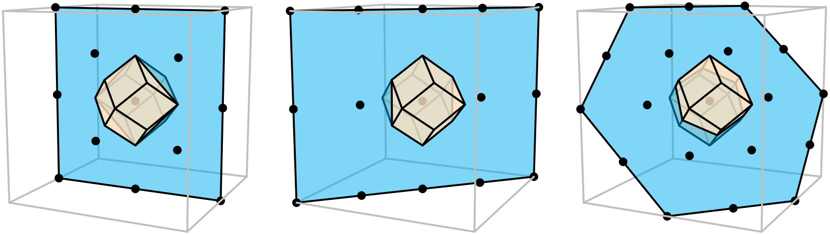

Spectra Visualization

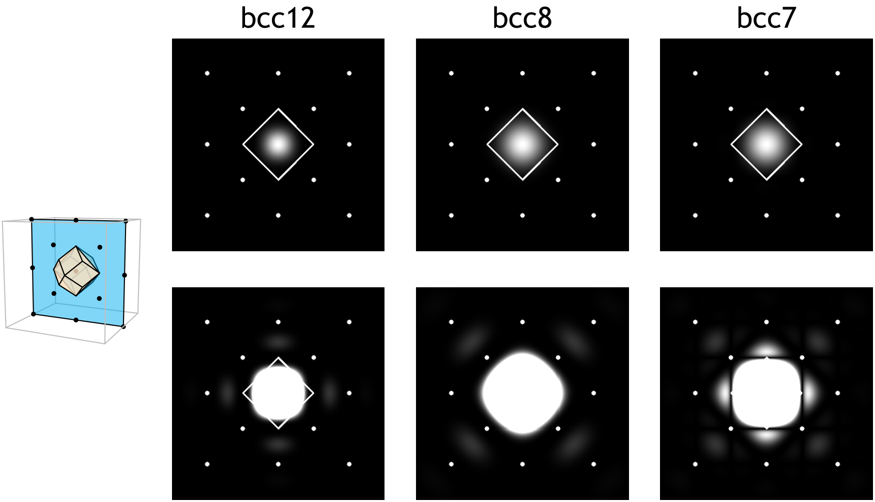

- Lower spectra are clamped to the range $[0, 0.0011]$.

Spectra Visualization

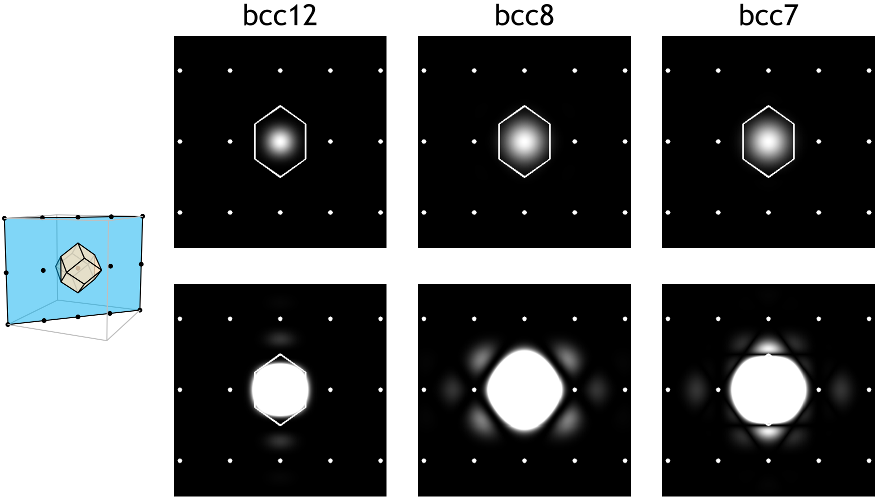

- Lower spectra are clamped to the range $[0, 0.0011]$.

Spectra Visualization

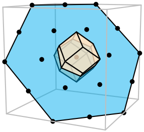

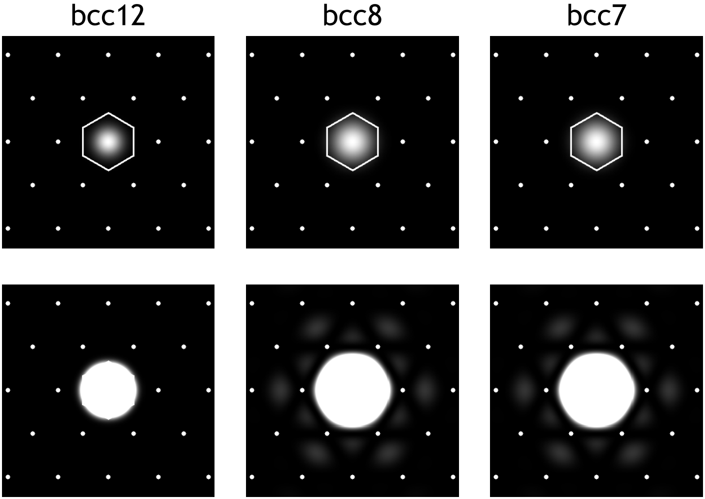

- Lower spectra are clamped to the range $[0, 0.0011]$.

Spectra Visualization

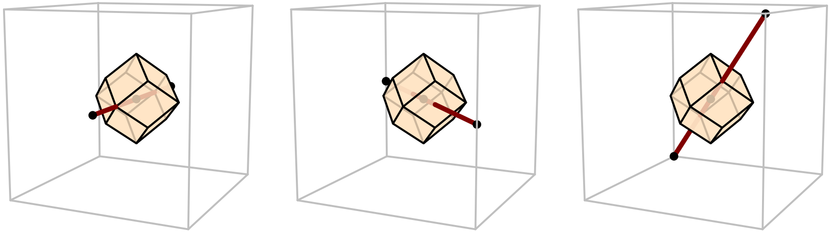

Spectra

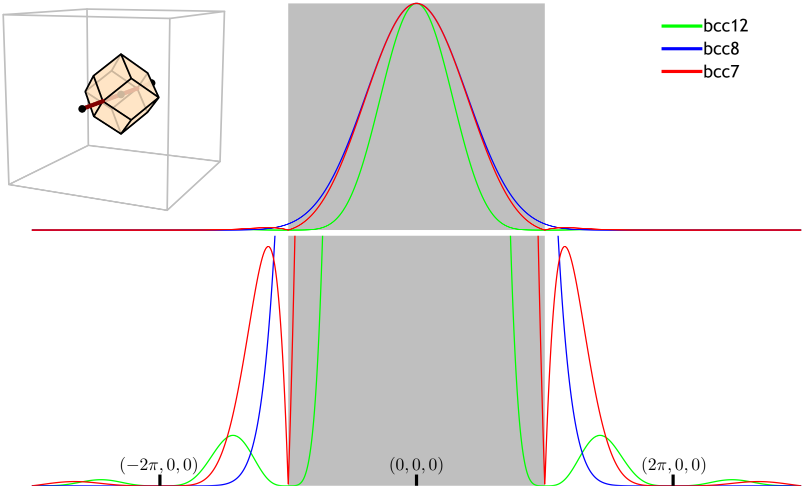

- Lower spectra are clamped to the range $[0, 0.0011]$.

Spectra

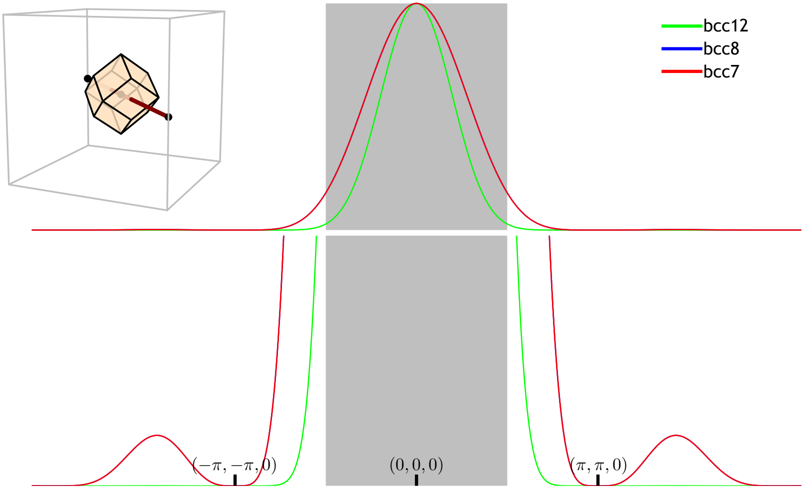

- Lower spectra are clamped to the range $[0, 0.0011]$.

Spectra

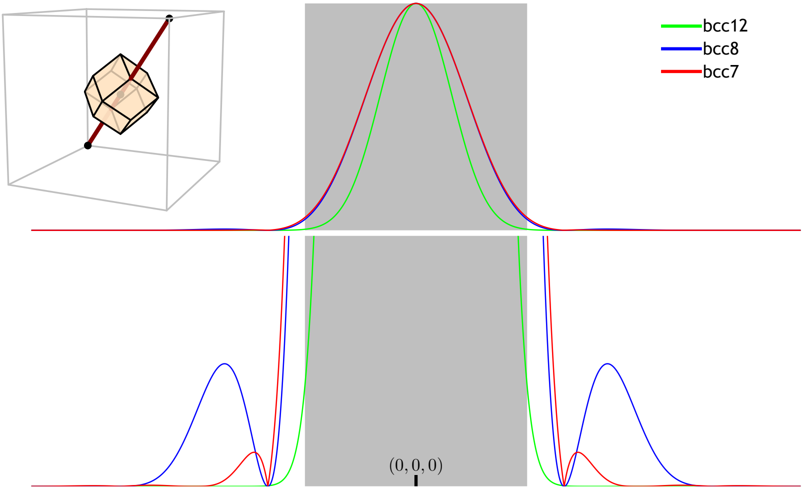

- Lower spectra are clamped to the range $[0, 0.0011]$.

Frequency Error Kernels

- Proposed by Blu and Unser [1999]

Frequency Error Kernels

- Proposed by Blu and Unser [1999]
- Average L_2 error according to sampling frequency ω

$$E(\omega) := \underbrace{1 - \frac{|\widehat{\phi}(\omega)|^2}{\widehat{a_\phi}(\omega)}}_{E_{\text{min}}(\omega)} + \underbrace{\widehat{a_\phi}(\omega)\left| Q(e^{j\omega}) - \frac{\widehat{\phi}^*(\omega)}{\widehat{a_\phi}(\omega)} \right|^2}_{E_{\text{res}}(\omega)}$$

Frequency Error Kernels

- Proposed by Blu and Unser [1999]
- Average L_2 error according to sampling frequency ω

$$E(\omega) := \underbrace{1 - \frac{|\widehat{\phi}(\omega)|^2}{\widehat{a_\phi}(\omega)}}_{E_{\text{min}}(\omega)} + \underbrace{\widehat{a_\phi}(\omega)\left|Q(e^{j\omega}) - \frac{\widehat{\phi}^*(\omega)}{\widehat{a_\phi}(\omega)}\right|^2}_{E_{\text{res}}(\omega)}$$

  - $\widehat{a_\phi}$: *autocorrelation* function of ϕ

Frequency Error Kernels

- Proposed by Blu and Unser [1999]
- Average L_2 error according to sampling frequency $\boldsymbol{\omega}$

$$E(\boldsymbol{\omega}) := \underbrace{1 - \frac{|\widehat{\phi}(\boldsymbol{\omega})|^2}{\widehat{a_\phi}(\boldsymbol{\omega})}}_{E_{\mathrm{min}}(\boldsymbol{\omega})} + \underbrace{\widehat{a_\phi}(\boldsymbol{\omega}) \left| Q(e^{j\boldsymbol{\omega}}) - \frac{\widehat{\phi}^*(\boldsymbol{\omega})}{\widehat{a_\phi}(\boldsymbol{\omega})} \right|^2}_{E_{\mathrm{res}}(\boldsymbol{\omega})}$$

  - $\widehat{a_\phi}$: *autocorrelation* function of ϕ
  - $Q(e^{j\boldsymbol{\omega}})$ is the discrete time Fourier transform of the prefilter $q(\boldsymbol{k})$,

Frequency Error Kernels

- Proposed by Blu and Unser [1999]
- Average L_2 error according to sampling frequency $\boldsymbol{\omega}$

$$E(\boldsymbol{\omega}) := \underbrace{1 - \frac{|\widehat{\phi}(\boldsymbol{\omega})|^2}{\widehat{a_\phi}(\boldsymbol{\omega})}}_{E_{\text{min}}(\boldsymbol{\omega})} + \underbrace{\widehat{a_\phi}(\boldsymbol{\omega}) \left| Q(e^{j\boldsymbol{\omega}}) - \frac{\widehat{\phi}^*(\boldsymbol{\omega})}{\widehat{a_\phi}(\boldsymbol{\omega})} \right|^2}_{E_{\text{res}}(\boldsymbol{\omega})}$$

  - $\widehat{a_\phi}$: *autocorrelation* function of ϕ
  - $Q(e^{j\boldsymbol{\omega}})$ is the discrete time Fourier transform of the prefilter $q(\boldsymbol{k})$,
- Can be computed by evaluating a box-spline filter on the lattice points.

Frequency Error Kernels

- Optimal error kernels

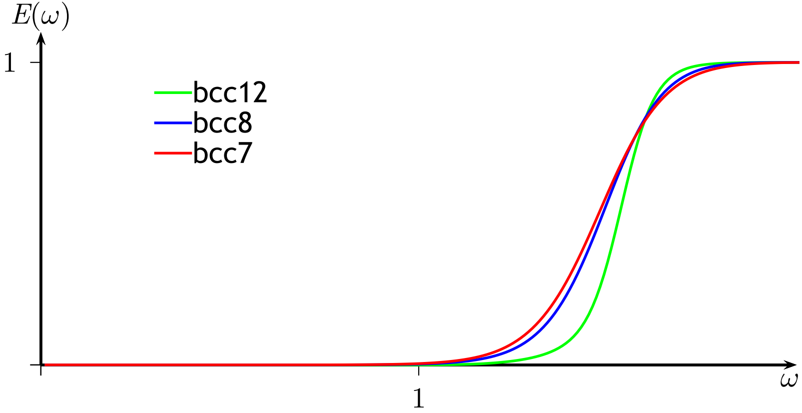

Frequency Error Kernels

- Without prefiltering

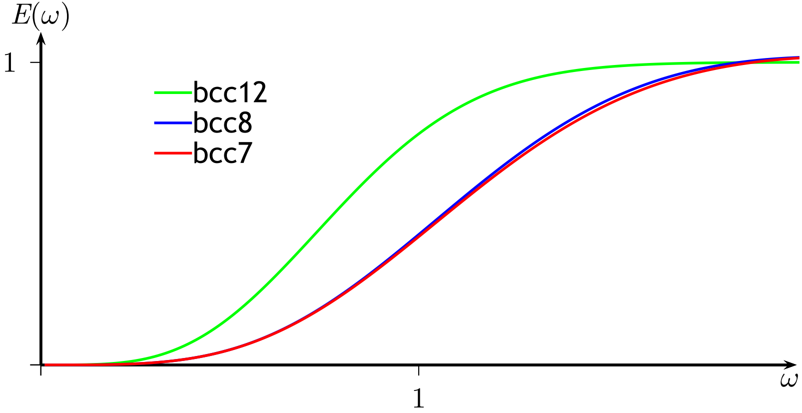

Frequency Error Kernels

- With quasi-interpolation prefilter of type I

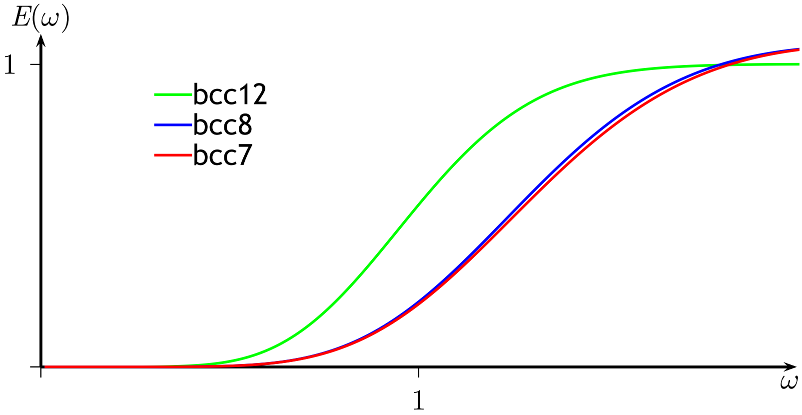

Frequency Error Kernels

- With quasi-interpolation prefilter of type II

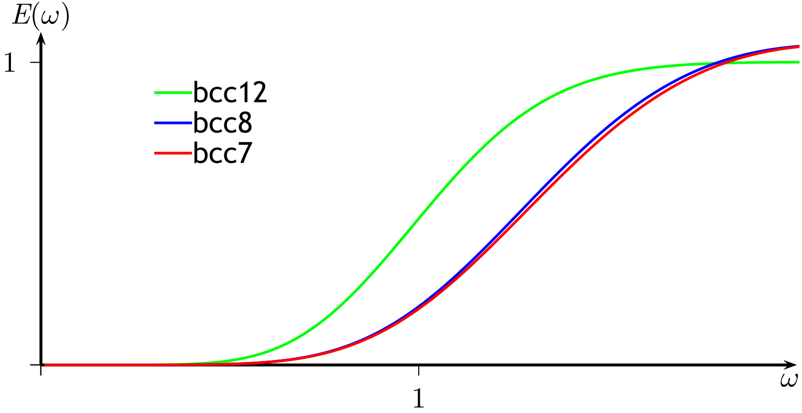

Frequency Error Kernels

- Optimal error kernels

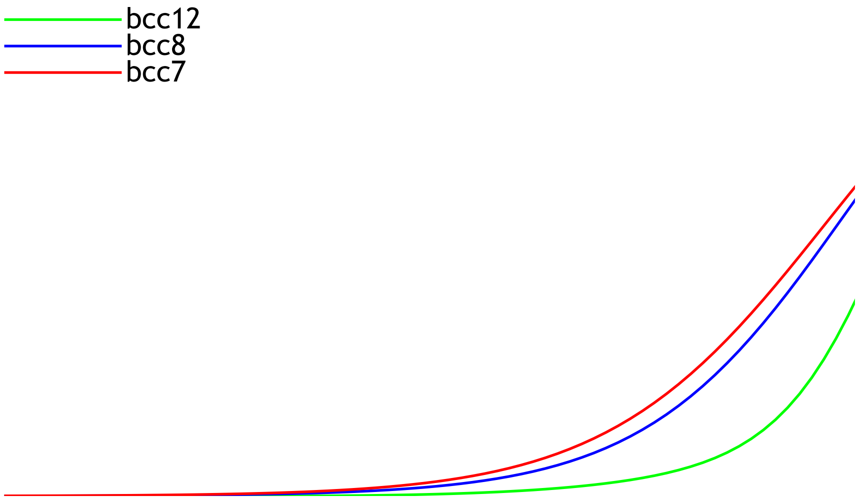

Frequency Error Kernels

- Without prefiltering

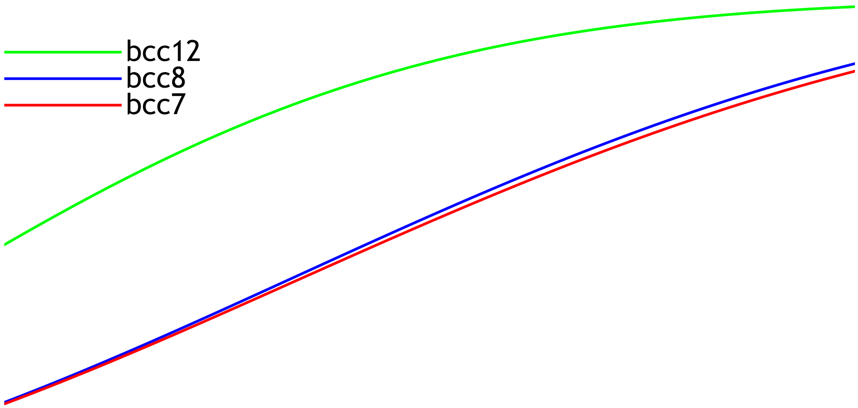

Frequency Error Kernels

- With quasi-interpolation prefilter of type I

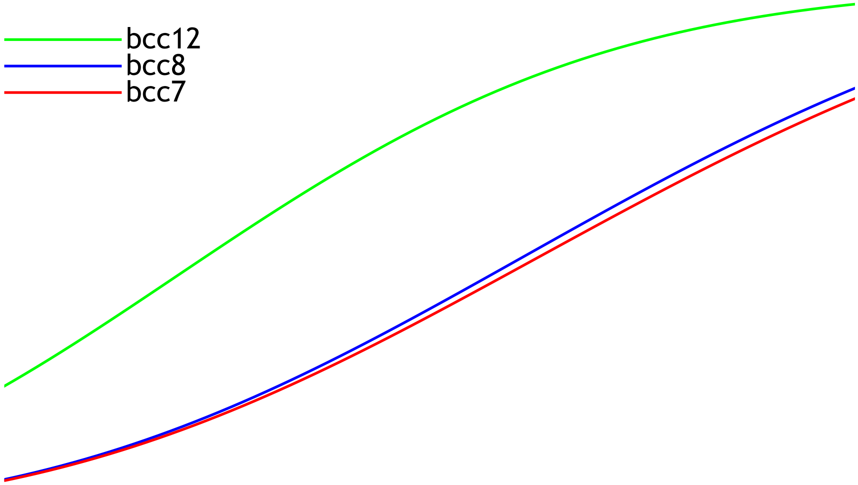

Frequency Error Kernels

- With quasi-interpolation prefilter of type II

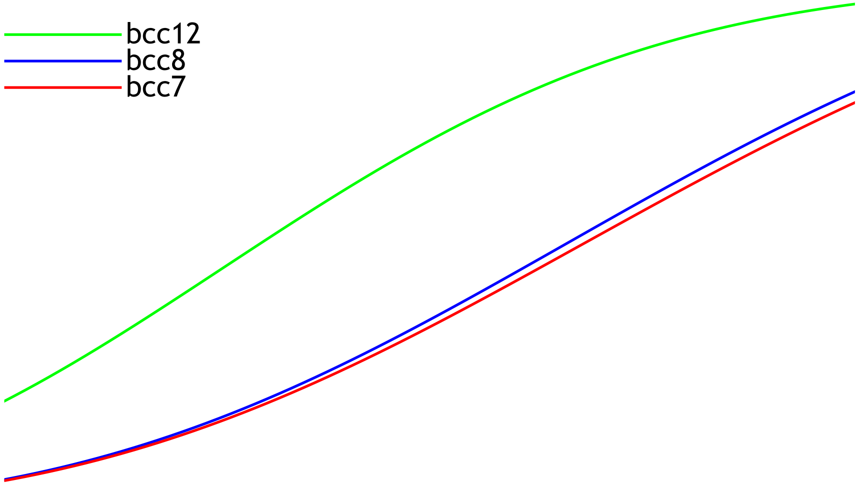

Quality Comparison

Quality Comparison

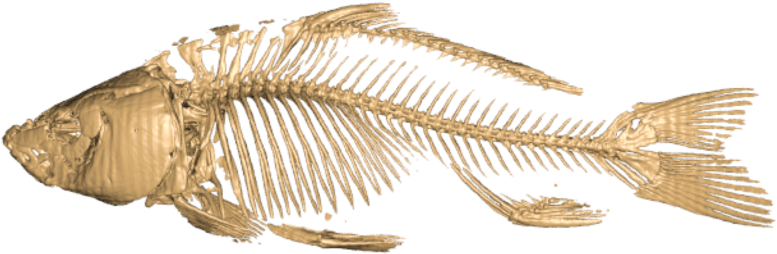

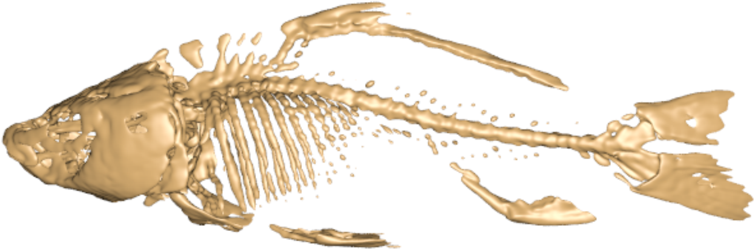

Quality Comparison: bcc12 vs. bcc8 vs. bcc7 (cont'd)

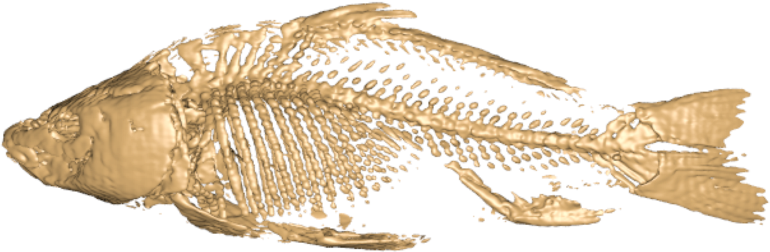

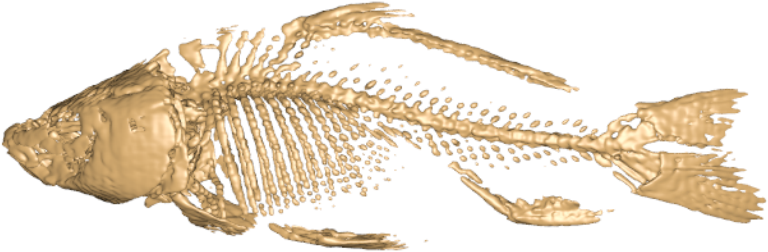

ML Datasets

ML Datasets

- Proposed by Marschner and Lobb [1994]

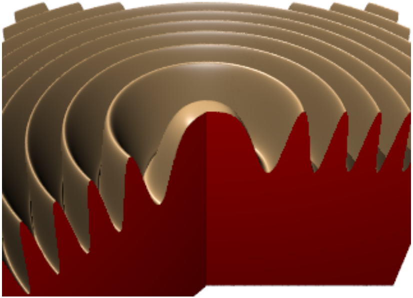

ML Datasets

- # of samples: $39^3 \times 2$

bcc12

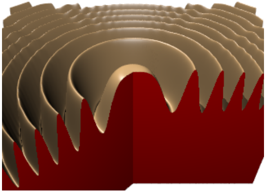

bcc8

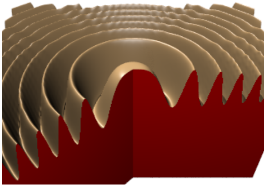

bcc7

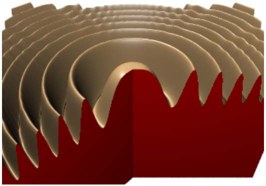

ML Datasets

- # of samples: $31^3 \times 2$

bcc12 bcc8 bcc7

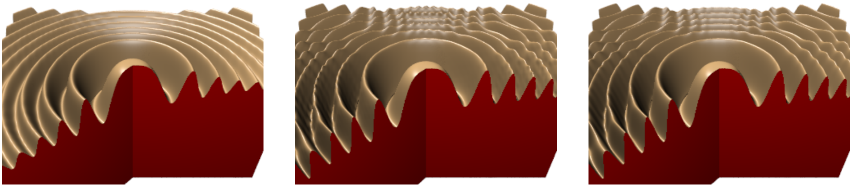

ML Datasets

- # of samples: $27^3 \times 2$

bcc12

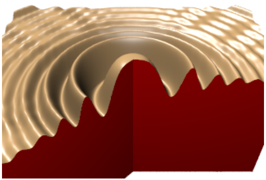

bcc8

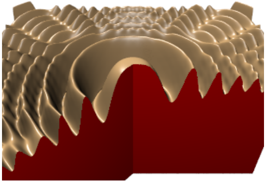

bcc7

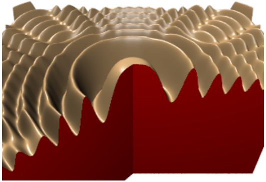

ML Datasets

- # of samples: $23^3 \times 2$

bcc12

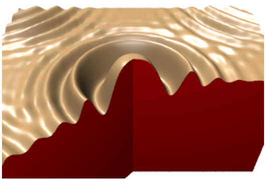

bcc8

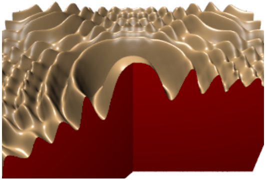

bcc7

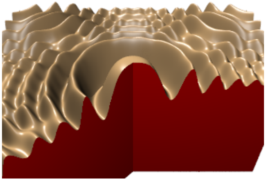

ML Datasets

- # of samples: $19^3 \times 2$

bcc12

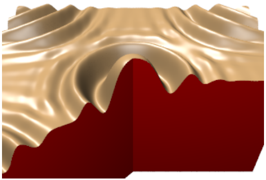

bcc8

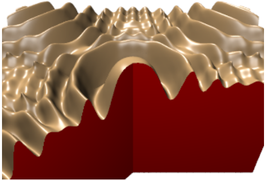

bcc7

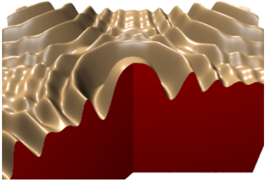

ML Datasets (Close-Up): bcc8 vs. bcc7

- $39^3 \times 2$

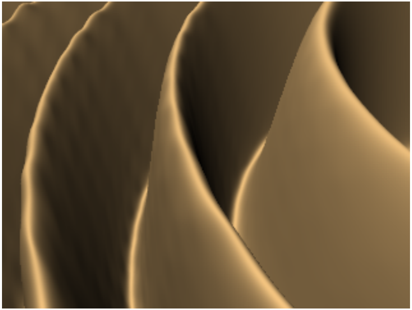

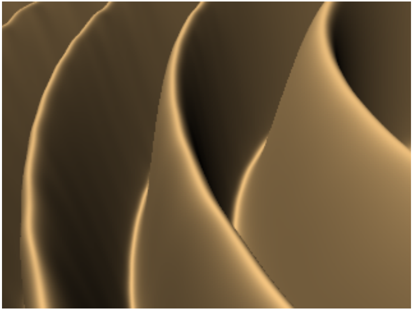

ML Datasets (Close-Up): bcc8 vs. bcc7

- $31^3 \times 2$

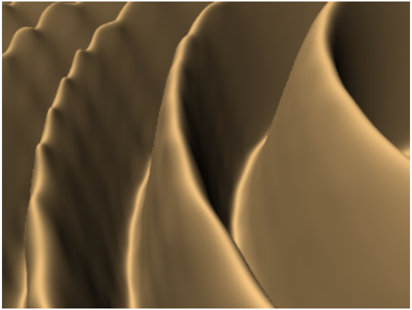

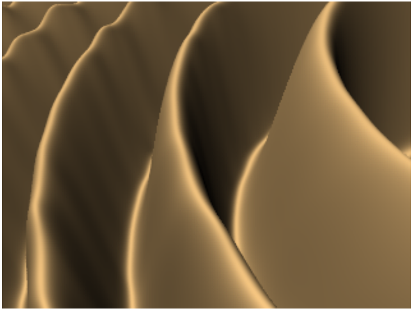

ML Datasets (Close-Up): bcc8 vs. bcc7

- $27^3 \times 2$

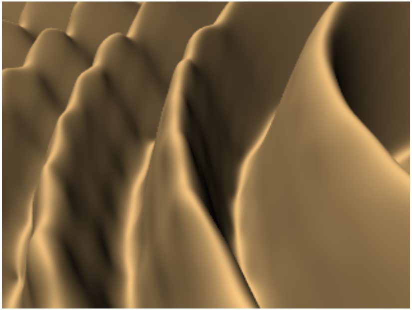

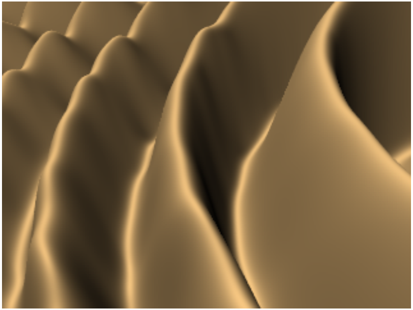

ML Datasets (Close-Up): bcc8 vs. bcc7

- $23^3 \times 2$

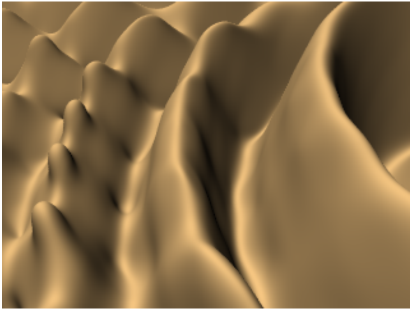

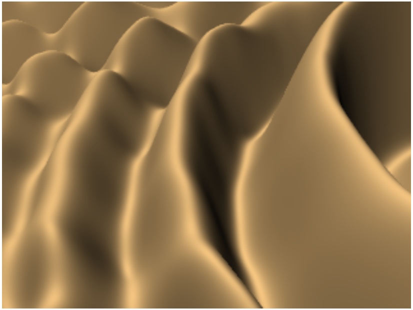

Quality Comparison (bcc8 vs. bcc7)

Quality Comparison (bcc8 vs. bcc7)

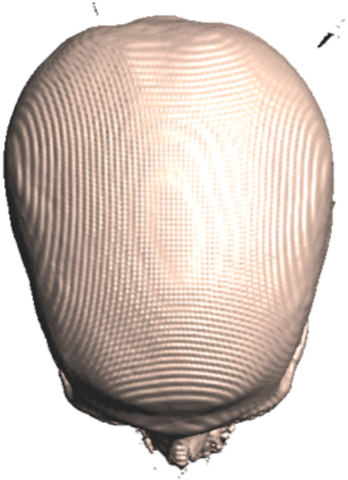

Quality Comparison (bcc8 vs. bcc7)

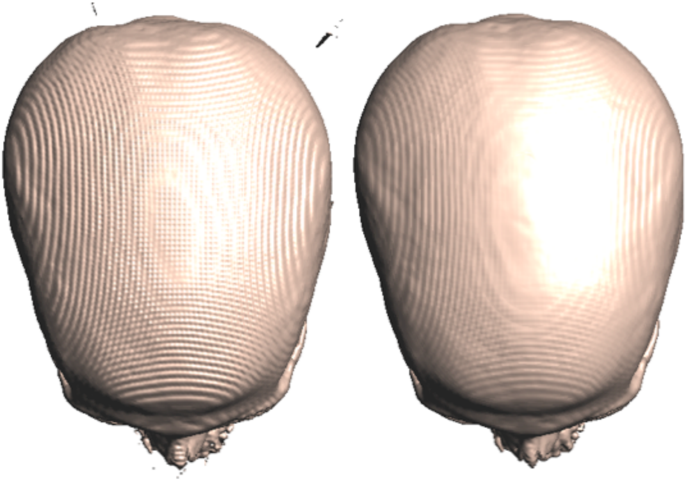

Quality Comparison (bcc8 vs. bcc7)

Quality Comparison (bcc8 vs. bcc7)

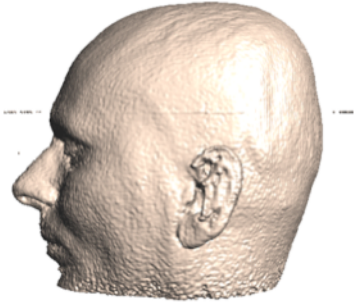

Quality Comparison (bcc8 vs. bcc7)

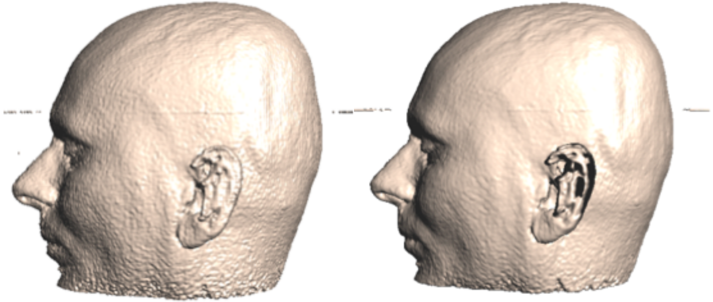

Outline

Conclusion and Future Work

Conclusion and Future Work

Conclusion

Conclusion and Future Work

Conclusion

- A novel reconstruction scheme on the BCC lattice with

Conclusion and Future Work

Conclusion

- A novel reconstruction scheme on the BCC lattice with
  - better approximation power and

Conclusion and Future Work

Conclusion

- A novel reconstruction scheme on the BCC lattice with
  - better approximation power and
  - efficient evaluation.

Conclusion and Future Work

Conclusion

- A novel reconstruction scheme on the BCC lattice with
  - better approximation power and
  - efficient evaluation.

Future Work

Conclusion and Future Work

Conclusion

- A novel reconstruction scheme on the BCC lattice with
  - better approximation power and
  - efficient evaluation.

Future Work

- GPU ray-caster

Conclusion and Future Work

Conclusion

- A novel reconstruction scheme on the BCC lattice with
  - better approximation power and
  - efficient evaluation.

Future Work

- GPU ray-caster
- Analysis of gradient error

Conclusion and Future Work

Conclusion

- A novel reconstruction scheme on the BCC lattice with
  - better approximation power and
  - efficient evaluation.

Future Work

- GPU ray-caster
- Analysis of gradient error
- Improved quasi-interpolation prefilter

Outline

References I

T. Blu and M. Unser. Quantitative Fourier analysis of approximation techniques: Part I – interpolators and projectors. *IEEE Transactions on Signal Processing*, 47(10): 2783 – 2795, Oct. 1999.

B. Csébfalvi and M. Hadwiger. Prefiltered B-spline reconstruction for hardware-accelerated rendering of optimally sampled volumetric data. In *Vision, Modeling, and Visualization*, pages 325–332, 2006.

C. de Boor, K. Höllig, and S. Riemenschneider. *Box splines*. Springer-Verlag New York, Inc., 1993.

A. Entezari, R. Dyer, and T. Möller. Linear and cubic box splines for the body centered cubic lattice. In *Proceedings of the IEEE Conference on Visualization*, pages 11–18. IEEE Computer Society, 2004.

References II

M. Kim, A. Entezari, and J. Peters. Box spline reconstruction on the face-centered cubic lattice. *IEEE Transactions on Visualization and Computer Graphics*, 14(6):1523–1530, Nov.-Dec. 2008.

S. R. Marschner and R. J. Lobb. An evaluation of reconstruction filters for volume rendering. In *Proceedings of the IEEE Conference on Visualization*, pages 100–107, Oct. 1994. doi: 10.1109/VISUAL.1994.346331.

J. Peters. C^2 surfaces built from zero sets of the 7-direction box spline. In *IMA Conference on the Mathematics of Surfaces*, pages 463–474, 1994.

D. P. Petersen and D. Middleton. Sampling and reconstruction of wave-number-limited functions in N-dimensional Euclidean spaces. *Information and Control*, 5(4):279–323, 1962.